AN X-RAY ABSORPTION FINE STRUCTURE SPECTROSCOPY STUDY OF METAL SORPTION TO GRAPHENE OXIDE

Supplementary Material

Allison R. Showalter[a], Thomas A. Duster[b], Jennifer E. S. Szymanowski[b], Chongzheng Na[b], Jeremy B. Fein[b*], and Bruce A. Bunker[a]

[a] Department of Physics, 225 Nieuwland Science Hall, University of Notre Dame, Notre Dame, IN 46556, USA

[b] Department of Civil and Environmental Engineering and Earth Sciences, 156 Fitzpatrick Hall, University of Notre Dame, Notre Dame, IN 46556, USA

*Corresponding Author/Current Details: Jeremy Fein/ fein@nd.edu

Other correspondence details (respectively):

thomas.duster@nist.gov / jszymanowski@nd.edu / cna@nd.edu / bunker@nd.edu / ashowal1@nd.edu

S.1 SYNTHESIS AND CHARACTERIZATION OF GRAPHENE OXIDE PARTICLES

Multi-layered graphene oxide (MLGO) particles were synthesized from natural flake graphite (Alfa Aesar, 99.9995%) using the method of Hummers and Offeman [1]. Concentrations are as given in the paper, but the overall process can be summarized as follows. Graphite was mixed in an ice bath with $NaNO_3$, H_2SO_4, and $KMnO_4$, then transferred to a water bath at ~35 °C and stirred for 30 minutes. After that, ultrapure water (R>18 MΩ cm, TOC < 2 μgC L^{-1}) was added to the mixture and stirred for ~20 minutes. All residual permanganate was then reacted and consumed by adding 30% H_2O_2. After that, the suspension was centrifuged, decanted, washed and rinsed repeatedly with 1.2 N HCl and ultrapure water before collection of MLGO via centrifugation. The end product was freeze-dried under vacuum for 5-7 days before use.

The resulting dried mass was partitioned and dispersed in ultrapure water using end-over-end rotation for about 3 hours. After particles were fully suspended, they were concentrated to ensure multiple layered particles only by repeated sedimentation. This was completed by centrifuging (4000g for 5 minutes), decanting the supernatant, and re-suspending the pellet in clean ultrapure water. The single or few layered nanosheets remained suspended even after centrifugation and were removed in the decanted supernatant. Final suspension concentrations were determined using the difference between the wet and dry (105 °C for >24 hours) masses of 20 mL replicate samples. The average concentration of the stock suspensions were ~2 g of MLGO per L of solution, with final pH value falling between 2.8 and 3.2.

Characterization of the MLGO particles was completed using atomic force microscopy (AFM; XE-70, Park Systems, Santa Clara, CA). Samples from the MLGO stock suspensions were diluted with ethanol in a 1:4 MLGO:ethanol ratio and deposited on freshly cleaved mica.

The instrument was operated in non-contact mode and images were flattened using the WSxM software package from Nanotec Electronica S.L. (Madrid, Spain). Resultant AFM analyses determined the height in the z-direction, from which the extent of exfoliation present in the sample can be inferred using MLGO layer height. Heights of up to 10 nm were acquired for the MLGO particles, as shown in Fig. S.1.

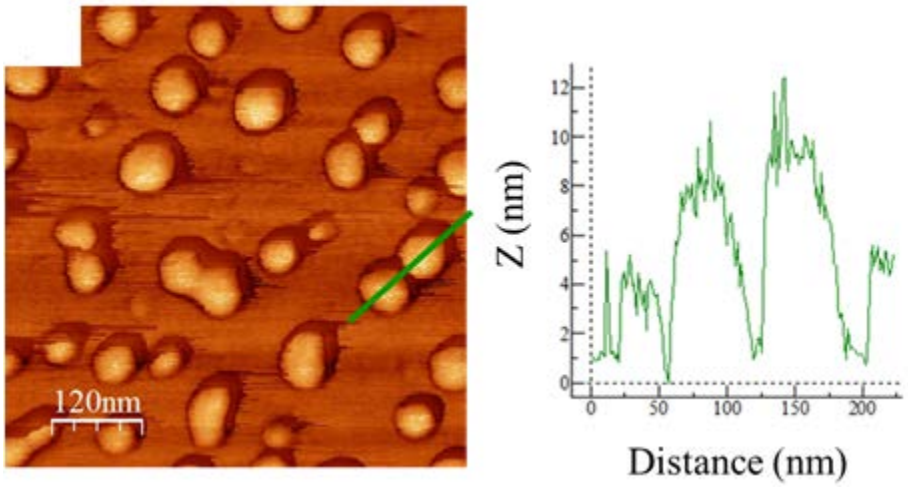

Fig. S.1: AFM image and height profile for the indicated cross-section in green for MLGO particles. Reprinted from Colloids and Surfaces A, 466, T.A. Duster, et al., "Surface complexation modeling of proton and metal sorption onto graphene oxide," 28-39, 2015, with permission from Elsevier [2].

S.2 ADDITIONAL DETAILS ON X-RAY ABSORPTION FINE STRUCTURE SAMPLE PREPARATION AND MEASUREMENTS

As discussed in the main text, solution standards were made by dissolving commercial metal nitrate salts in water to a concentration of 10 mM metal ion with 100 mM ligand ion and pH adjusted to appropriate values for desired complexation using ≤ 1 M HNO_3 or NaOH . Ligands for solution standards include perchlorate (added as sodium perchlorate), acetate (added as sodium acetate) and ethylenediaminetetraacetate (added as ethylenediaminetetraacetic acid [EDTA]) or salicylate (added as sodium salicylate). Cd-perchlorate was adjusted to pH 3.0, Cd-

EDTA was set to pH 5.0 and Cd-acetate was raised to pH 4.5. U-perchlorate was adjusted to pH 2.0, U-salicylate was set to 4.0 and U-acetate was raised to pH 5.5. Finally, Pb-perchlorate was adjusted to pH 3.0, Pb-EDTA was set to pH 6.4 and Pb-acetate was raised to pH 5.0.

Cd K edge (26,711 eV), U L(III) edge (17,166 eV) and Pb L(III) edge (13,035 eV) XAFS measurements were collected at the Sector 10 Materials Research Collaborative Access Team (MR-CAT) insertion device (ID) beamline [3] or bending magnet (BM) beamline [4] at the Advanced Photon Source (APS) at Argonne National Laboratory (USA). All samples and standards were measured at room temperature, with solid standards measured in transmission and experimental samples and solution standards measured in fluorescence using the Stern-Heald geometry [5]. The incident X-ray beam energy was scanned using the Si(III) reflection plane of a cooled double-crystal monochromator. A Pt-coated mirror was used to reject the higher harmonics from the Si crystal at the Cd K edge and a Rh-coated mirror was used to reject the higher harmonics from the Si crystal at the U L(III) and Pb L(III) edges. Undulator parameters at the ID line were set to optimize the energy intensity profile as follows: third harmonic and taper of about 3.5 keV for the Cd K edge, second harmonic and taper of about 3.0 keV for the U L(III) edge, and second harmonic and taper of about 2.5 keV for the Pb L(III) edge.

At both the ID and BM lines, the incident ion chamber was filled with inert gas (N_2 for Cd, U and Pb), the transmitted and reference ion chambers were filled with inert gas (Ar for Cd, 75% Ar/25% N_2 for U and 50% Ar/50% N_2 for Pb) and the fluorescence Lytle detector was filled with inert gas (Kr for Cd, Ar for U and Pb). The incident X-ray beam was reduced to 1.0 mm^2 using 1 mm x 1 mm slits. About 30-75 total quick scans were merged for each sample at the ID line, with a 0.1 s integration time taken in 0.5 eV steps over the scan range (200 eV below edge energy to 1000 eV above edge energy for Cd and U and 800 eV above edge energy for Pb), or

about a 3-4 minute scan. About 3-15 step scans (~20 minute scans) were averaged for samples and standards at the BM line. At both lines, a cadmium foil, uranyl nitrate powder standard or lead foil (foils commercially available from the EXAFS Company) was placed in front of the reference ionization chamber and the first inflection point of the resulting XAFS scan was set to 26,711 eV for Cd; 17,166 eV for U and 13,035 for Pb and used to align the scans of all samples and standards.

S.3 RESULTS FOR ICP-OES OF METAL SORPTION TO MLGO SAMPLES

For all inductively coupled plasma optical emission spectroscopy (ICP-OES) measurements, the initial (C_0) and final (C_f) solution metal concentrations were measured and the adsorbed metal percentage was calculated using

$$\%\ adsorbed = \frac{C_0 - C_f}{C_0} \times 100\% \quad \text{(S.1)}$$

with results listed in Table S.1. All listed results fall within previous batch adsorption curve results from Duster et al. 2015 [2].

Table S.1

ICP-OES Results for Amount of Cd(II), U(VI) or Pb(II) Adsorbed to MLGO

Sample	pH	% adsorbed
Cd-MLGO	4.9	15
	6.4	60
	8.1	80
U-MLGO	4.0	79
	5.8	97
	7.2	97
	8.5	88
Pb-MLGO	5.0	91
	6.0	100
	6.8	100
	8.3	100

S.4 ADDITIONAL XAFS RESULTS FOR CD(II) STANDARDS AND SAMPLES

The fitting result parameters for Cd(II) aqueous solution standards are listed in Table 1 of the main text. The fits for the hydrated Cd^{+2} ion, Cd-EDTA and Cd-acetate are shown in Fig. S.2, along with a sample of path contributions from the Cd-acetate data. In addition, Fig. S.3 shows a theoretical fit with two Cd-C paths that destructively interfere to produce almost no Cd-C EXAFS signature. Note how the total fit is nearly identical to the Cd-O path alone.

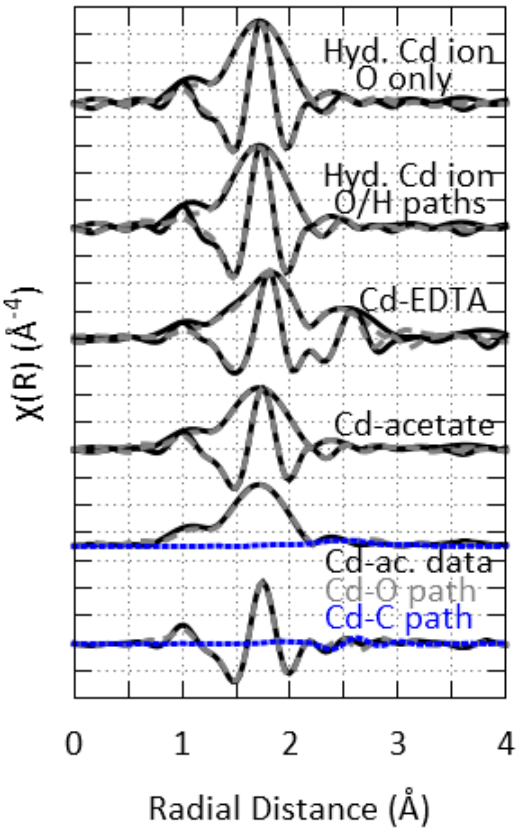

Fig. S.2: Fourier transformed (FT) spectra of Cd(II) aqueous standard compounds showing both the magnitude (all positive) and real part of the data (solid black line) and the best fit line (dashed gray line). The bottom shows example fitting paths of the Cd-O path (dashed gray line) and the Cd-C path (dotted blue line) for the Cd-acetate fit (black line) in both magnitude (top) and real part (bottom) of the FT spectra.

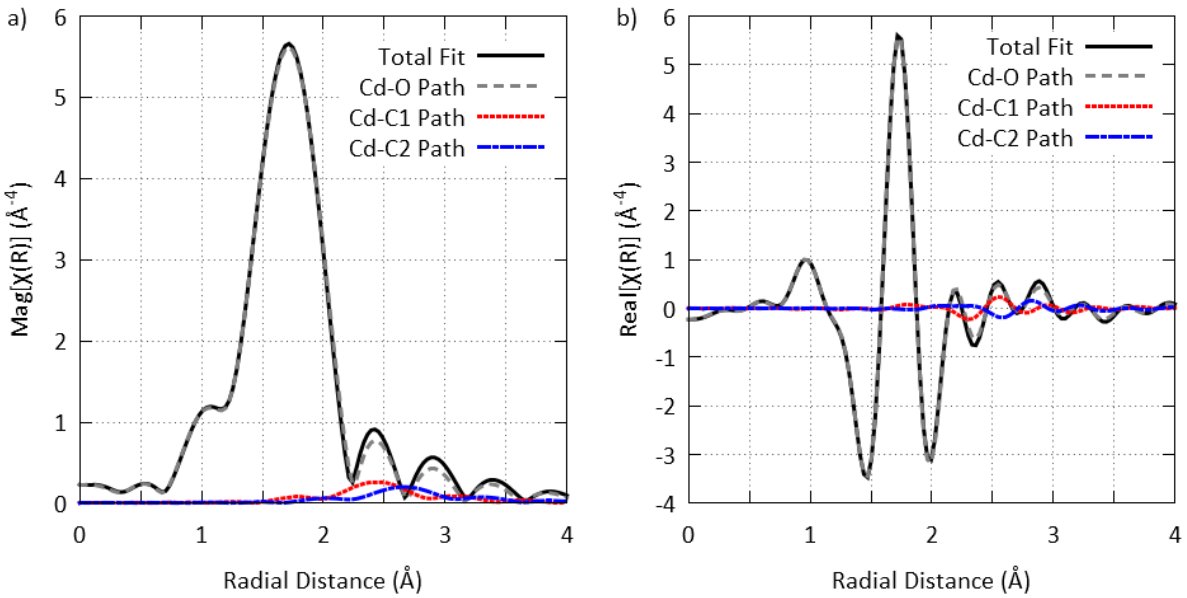

Fig. S.3: Contributing Cd-O (dashed gray line) and two Cd-C paths (dotted red line and dash-dot blue line) demonstrating possible destructive interference from multiple adsorption sites or a floppy monodentate inner sphere bond for a) the magnitude of the FT data (black line) and b) the real part of the FT data (black line). Note the strong similarities between the total fit and the Cd-O path, with the two Cd-C paths contributing almost nothing to the total fit across the fitting range.

S.5 ADDITIONAL XAFS RESULTS FOR U(VI) STANDARDS AND SAMPLES

The fitting result parameters for U(VI) aqueous solution standards are listed in Table 2 of the main text. The fits for the hydrated UO_2^{+2} ion, UO_2^{+2}-salicylate and UO_2^{+2}-acetate are shown in Fig. S.4, along with a sample of path contributions from the UO_2^{+2}-acetate data. Additional XANES data are shown in Fig. S.5a of the standards made from uranyl ions in solution at different pH values, while Fig. S.5b shows an uncluttered comparison of the U-MLGO samples at pH 4.0, 5.8, 7.2 and 8.5 in comparison with the hydrated UO_2^{+2} ion. Table S.2 lists a secondary fit with nearly identical goodness-of-fit parameters to those listed in Table 2 of the main text and fit results are shown in Fig. S.6. This fit of the U-MLGO data involves the

inclusion of a split equatorial oxygen shell, while the fit in the main text allows for only one equatorial oxygen shell.

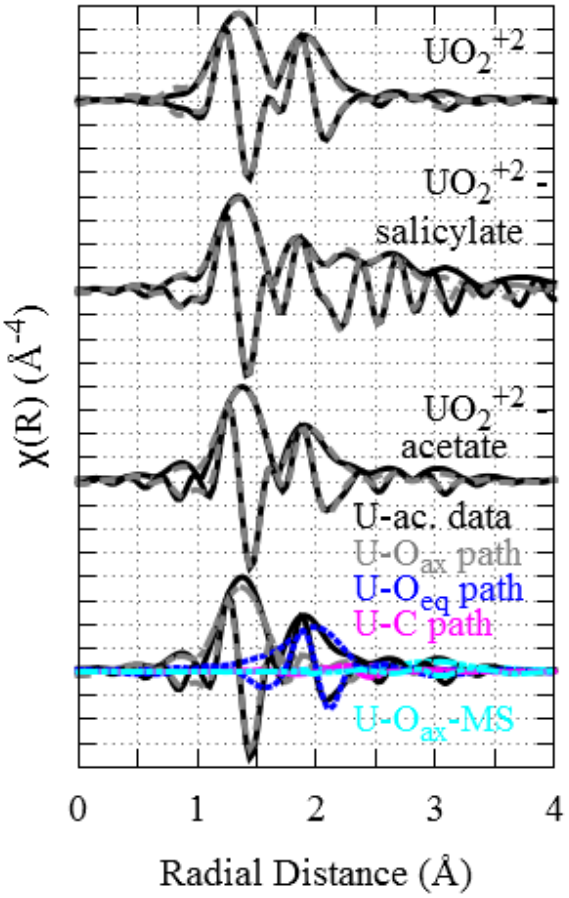

Fig. S.4: Fourier transformed (FT) spectra of U(VI) aqueous standard compounds showing both the magnitude (all positive) and real part of the data (solid black line) and the best fit line (dashed gray line). The bottom shows example fitting paths of the U-O_{ax} path (dashed gray line), the U-O_{eq} path (dotted blue line), the U-C path (dash-dot purple line) and the multiple scattering paths of the U-O_{ax} path (teal dot-dot-dash line) for the UO_2^{+2}-acetate fit (black line) in both the magnitude and the real part of the FT spectra.

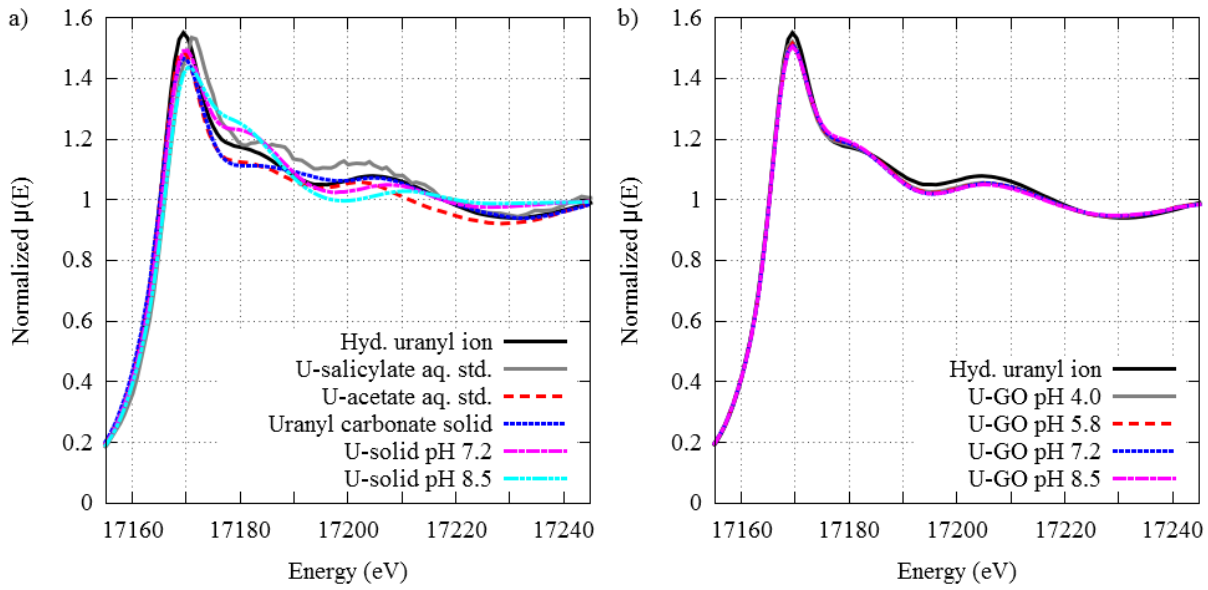

Fig. S.5: XANES data for U-MLGO data showing a) the solid and aqueous standards only and b) just the U-MLGO data at pH 4.0, 5.8, 7.2 and 8.5 with the UO_2^{+2} hydrated ion for comparison, [GO] = 0.42 g/L, [U] = 0.010 g/L, [$NaClO_4$] = 0.10 M, T = 293 K.

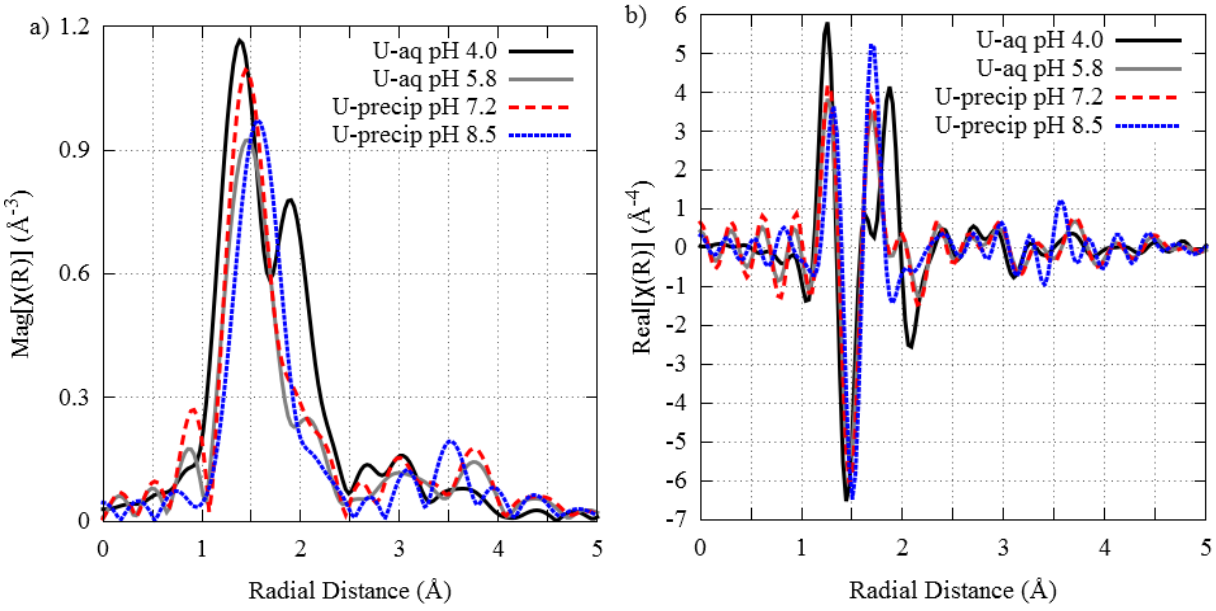

Fig. S.6: EXAFS data for U standards created at pH 4.0, 5.8, 7.2 and 8.5 showing a) the magnitude and b) the real part of the data, [U] = 0.010 g/L, [$NaClO_4$] = 0.10 M, T = 293 K.

Table S.2

EXAFS fitting parameters for U-MLGO samples using two equatorial oxygen shells.

Sample	Path	N	R (Å)	σ^2 (Å^2)	ΔE_o
U-MLGO	U-O_{ax}	2*	1.78 ± 0.01	0.002 ± 0.001	7.5 ± 2.1[a]
pH 4.0	U-O_{eq1}	2.7 ± 1.3	2.25 ± 0.02	0.010 ± 0.004	
	U-O_{eq2}	3.5 ± 1.3	2.56 ± 0.03	0.009 ± 0.003	8.0 ± 2.7[b]
	U-C	0.9 ± 0.7	3.05 ± 0.04	0.004 ± 0.005	
U-MLGO	U-O_{ax}	2*	1.78 ± 0.01	0.002 ± 0.001	7.5 ± 2.1[a]
pH 5.8	U-O_{eq1}	2.9 ± 1.4	2.25 ± 0.02	0.010 ± 0.004	
	U-O_{eq2}	3.7 ± 1.2	2.56 ± 0.03	0.009 ± 0.003	8.0 ± 2.7[b]
	U-C	1.0 ± 0.8	3.05 ± 0.04	0.004 ± 0.004	
U-MLGO	U-O_{ax}	2*	1.78 ± 0.01	0.002 ± 0.001	7.5 ± 2.1[a]
pH 7.2	U-O_{eq1}	2.6 ± 0.9	2.23 ± 0.03	0.010 ± 0.002	
	U-O_{eq2}	4.0 ± 1.4	2.56 ± 0.02	0.009 ± 0.004	8.0 ± 2.7[b]
	U-C	1.1 ± 0.8	3.05 ± 0.05	0.004 ± 0.006	
U-MLGO	U-O_{ax}	2*	1.78 ± 0.01	0.002 ± 0.001	7.5 ± 2.1[a]
pH 8.5	U-O_{eq1}	2.2 ± 0.9	2.24 ± 0.03	0.010 ± 0.002	
	U-O_{eq2}	4.3 ± 1.4	2.56 ± 0.03	0.009 ± 0.002	8.0 ± 2.7[b]
	U-C	1.7 ± 0.8	3.05 ± 0.03	0.004 ± 0.004	

*Coordination number for axial oxygen fixed to 2. [a]ΔE_o values for O_{ax} fixed to be same for U-MLGO samples. [b] ΔE_o values for O_{eq} and C paths fixed to be same for U-MLGO samples. N = coordination number, R = interatomic distance, σ^2 = Debye-Waller factor, ΔE_0 = energy shift

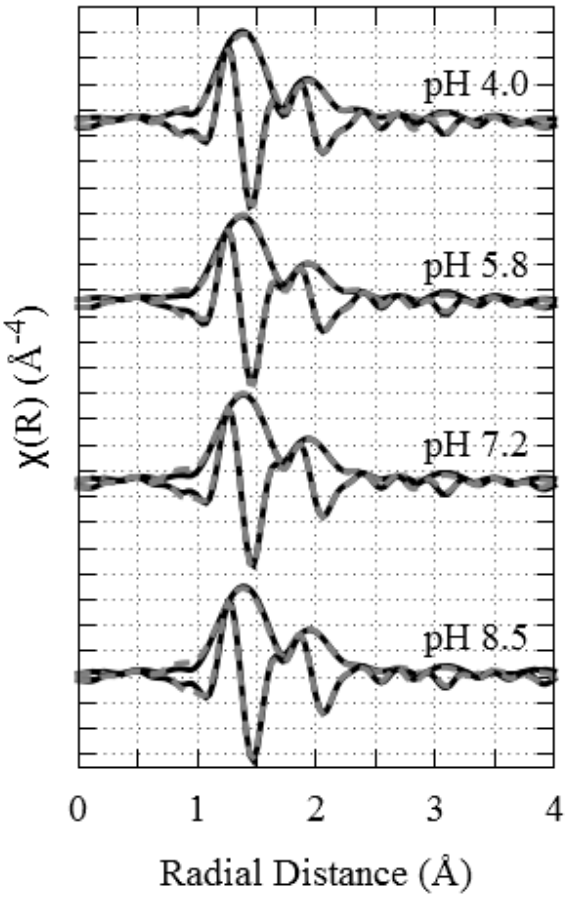

Fig. S.7: FT spectra of the U-MLGO samples at pH 4.0, 5.8, 7.2 and 8.5 with split equatorial oxygen shell showing both the magnitude (all positive) and real part of the data (solid black line) and the best fit line (dashed gray line), [GO] = 0.42 g/L, [U] = 0.010 g/L, [$NaClO_4$] = 0.10 M, T = 293 K.

S.4 ADDITIONAL XAFS RESULTS FOR PB(II) STANDARDS AND SAMPLES

The fitting result parameters for Pb(II) aqueous solution standards are listed in Table 3 of the main text. The fits for the hydrated Pb^{+2} ion, Pb-EDTA and Pb-acetate are shown in Fig. S.7. Examples of the path contributions in the pH 8.3 Pb-MLGO data set are shown in Fig. S.8. Additional XANES data showing the isosbestic points are shown in Fig. S.9a, while Fig. S.9b shows the real part of the FT spectra of these same samples.

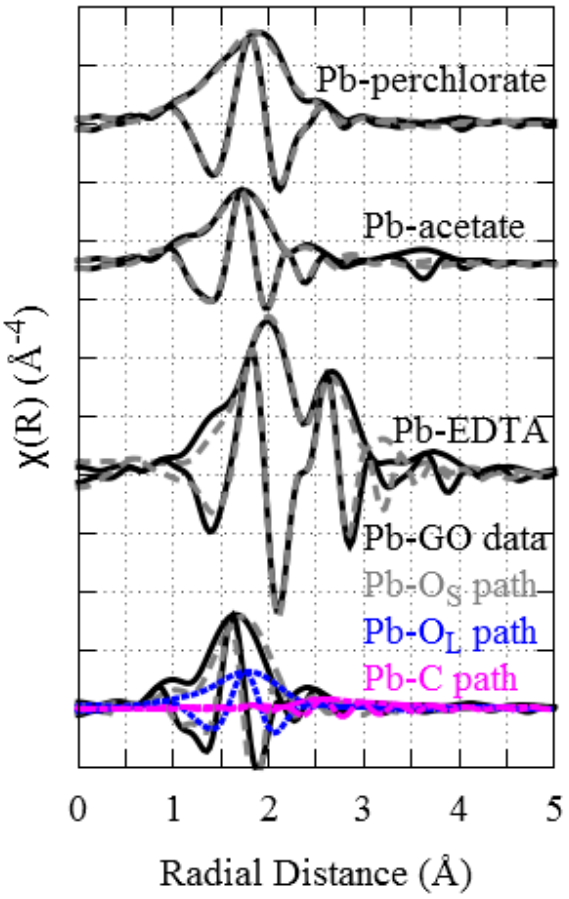

Fig. S.8: FT spectra of Pb(II) aqueous standard compounds showing both the magnitude (all positive) and real part of the data (solid black line) and the best fit line (dashed gray line).

The model used to describe the XAFS signal from the Pb-MLGO samples included single short and longer scattering paths for oxygen and a scattering path for carbon. All data were inconsistent with a model that included Pb neighbors or second nearest neighbors to the central Pb atom, indicating a negligible amount of Pb-bearing precipitate in the samples. The sample fits were conducted simultaneously, and since the lowest pH Pb-MLGO sample at pH 5.0 consistently yielded a coordination number of zero carbon atoms, that path was removed from the fit for that sample. The

presence of the isosbestic points and qualitative analysis of the EXAFS data indicated that there were likely two binding sites present in each sample, with the relative proportion of the two binding sites changing consistently as a function of pH. Therefore, the distances were constrained to be the same for each fitted sample. Initially, the Debye-Waller factors for all three paths and the third cumulant for the long oxygen path were allowed to be different for each sample within each path, but since all converged to the same values, they were restricted to be the same for all samples to allow for better restriction of uncertainties in the coordination numbers. Single sample fits agreed with the simultaneous fitting results, but due to the smaller number of free parameters, the simultaneous fit results were used to better constrain the coordination numbers.

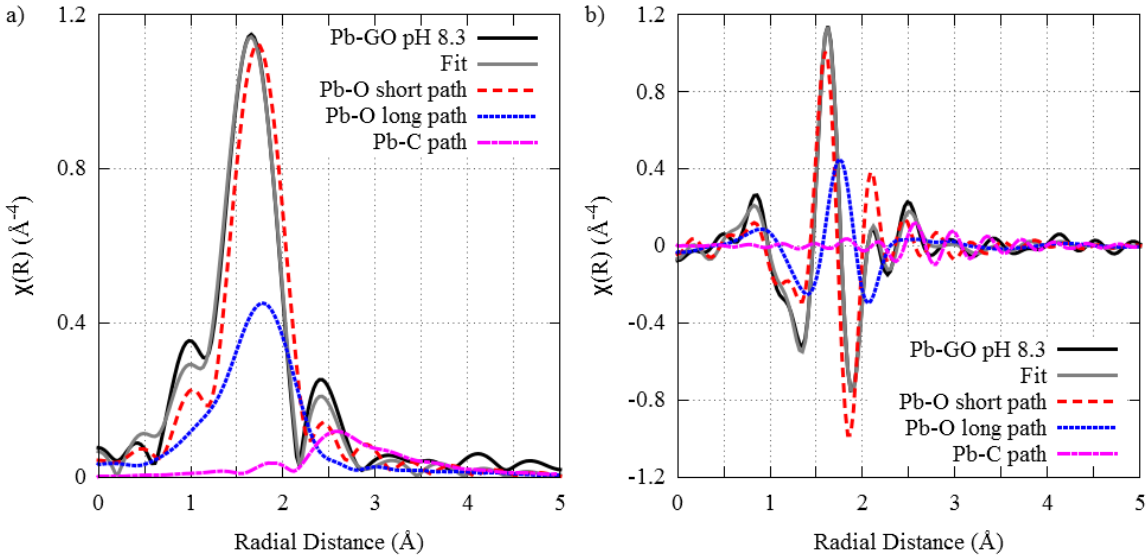

Fig. S.9: FT spectra and paths for the Pb-MLGO pH 8.3 data (black line) in both a) magnitude and b) real part with the fitting paths of the Pb-O_S path (dashed red line), the Pb-O_L path (dotted blue line) and the Pb-C path (dash-dot purple line) combining to form the total fit (gray line).

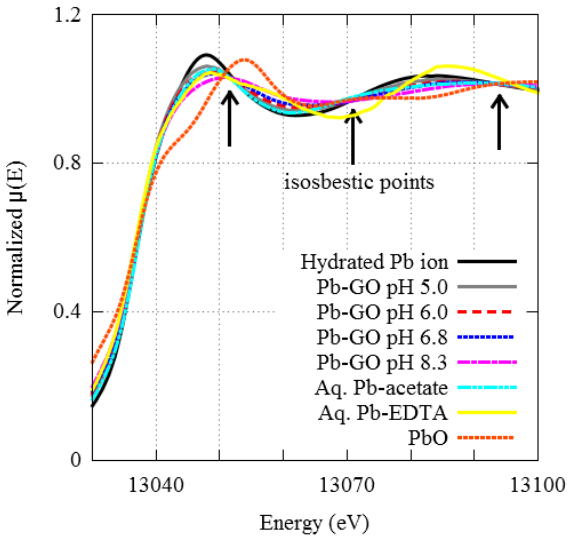

Fig. S.10: Comparison of Pb-MLGO sample data at pH 5.0, 6.0, 6.8 and 8.3 with the Pb aqueous standards and solid PbO in energy space for the near edge (XANES) region, with arrows indicating the isosbestic points, [GO] = 0.42 g/L, [Pb] = 0.010 g/L, [$NaClO_4$] = 0.10 M, T = 293 K.

Reference List

[1] W.S. Hummers, R.E. Offeman, Preparation of graphitic oxide, J. Am. Chem. Soc. 80 (1958) 1339-1339.

[2] T. Duster, C. Na, A. Showalter, B. Bunker, Surface complexation modeling of proton and metal sorption onto graphene oxide, Colloid Surf., A. 466 (2015) 28-39.

[3] C. Segre, N. Leyarovska, L. Chapman, W. Lavender, P. Plag, The MRCAT insertion device beamline at the Advanced Photon Source, Synchrotron Radiat. Instrum. 521 (2000) 419-422.

[4] A.J. Kropf, J. Katsoudas, S. Chattopadhyay, T. Shibata, E.A. Lang, V.N. Zyryanov, B. Ravel, K. McIvor, K.M. Kemner, K.G. Scheckel, S.R. Bare, J. Terry, S.D. Kelly, B.A. Bunker, C.U. Segre, R. Garrett, I. Gentle, K. Nugent, S. Wilkins, The new MRCAT (Sector 10) bending magnet beamline at the Advanced Photon Source, AIP Conf. Proc. 1234 (2010) 299-302.

[5] E. Stern, S. Heald, X-ray filter assembly for fluorescence measurements of X-ray absorption fine structure, Rev. Sci. Instrum. 50 (1979) 1579-1579.